The scaffold protein Ste5 directly controls a switch-like mating decision in yeast

Mohan K. Malleshaiah[1]*, Vahid Shahrezaei[3]*, Peter S. Swain[4,5] & Stephen W. Michnick[1,2]

Evolution has resulted in numerous innovations that allow organisms to increase their fitness by choosing particular mating partners, including secondary sexual characteristics, behavioural patterns, chemical attractants and corresponding sensory mechanisms[1]. The haploid yeast *Saccharomyces cerevisiae* selects mating partners by interpreting the concentration gradient of pheromone secreted by potential mates through a network of mitogen-activated protein kinase (MAPK) signalling proteins[2,3]. The mating decision in yeast is an all-or-none, or switch-like, response that allows cells to filter weak pheromone signals, thus avoiding inappropriate commitment to mating by responding only at or above critical concentrations when a mate is sufficiently close[4]. The molecular mechanisms that govern the switch-like mating decision are poorly understood. Here we show that the switching mechanism arises from competition between the MAPK Fus3 and a phosphatase Ptc1 for control of the phosphorylation state of four sites on the scaffold protein Ste5. This competition results in a switch-like dissociation of Fus3 from Ste5 that is necessary to generate the switch-like mating response. Thus, the decision to mate is made at an early stage in the pheromone pathway and occurs rapidly, perhaps to prevent the loss of the potential mate to competitors. We argue that the architecture of the Fus3–Ste5–Ptc1 circuit generates a novel ultrasensitivity mechanism, which is robust to variations in the concentrations of these proteins. This robustness helps assure that mating can occur despite stochastic or genetic variation between individuals. The role of Ste5 as a direct modulator of a cell-fate decision expands the functional repertoire of scaffold proteins beyond providing specificity and efficiency of information processing[5,6]. Similar mechanisms may govern cellular decisions in higher organisms and be disrupted in cancer.

The two haploid forms of *S. cerevisiae*, *MAT**a*** and *MATα*, secrete **a**- and α-factor pheromones respectively, which bind to pheromone-specific receptors and activate a canonical MAPK cascade (Fig. 1a). Cells respond by differentiating into several morphological states depending on the local concentration of pheromone. At a critical concentration most differentiate into shmoos, a pre-fusion state in which two cells of opposite mating type become close enough to form diploid cells[4,7,8] (Fig. 1a, b and Supplementary Fig. 2). At any concentration of pheromone, different morphological phenotypes coexist, but shmooing is an all-or-none response[4] (Fig. 1b and Supplementary Fig. 3). It is not known how switch-like shmooing is generated, but activation of the MAPK Fus3 is switch-like, suggesting that the switch is generated upstream or in the MAPK cascade[8] (Supplementary Fig. 4).

Disrupting the interaction between Fus3 and Ste5 using an Ste5[ND] mutant surprisingly relieves an inhibition of the mating response[9] and is sufficient to destroy switch-like shmooing (Fig. 1c). Hence, we reasoned that the switch could be generated by modulating this interaction. Ste5[ND] has a disrupted Fus3-docking motif (FDM), which prevents its binding to Fus3 (ref. 9). With Ste5[ND], the activation of Fus3 becomes graded and, fitting a Hill function to the data in Fig. 1b and c, we observe a Hill coefficient of ~9 for wild type versus 1 for Ste5[ND] (Supplementary Figs 3 and 4). The Fus3 homologue Kss1 does not contribute to switch-like shmooing[8] (Supplementary Figs 4–6).

Direct measurement of the steady-state levels of the Fus3–Ste5 complex showed a switch-like dissociation of the complex over the same range of concentrations of α-factor for which shmooing occurred (Hill coefficient of 6; half-maximum effective concentration (EC$_{50}$) of 0.15 μM) (Figs 1b and 2a). We measured the levels of the Fus3–Ste5 complex using a protein-fragment complementation assay based on *Renilla reniformis* (Rluc) luciferase as a reporter that detects interactions among proteins expressed endogenously without significantly altering their binding kinetics[10] (Supplementary Fig. 7 and see Supplementary Information). The Hill coefficient for our protein-fragment complementation assay results (~6) is smaller than that of the single cell response (~9; Supplementary Fig. 3), partly because the assay measures an average over a population of cells[11]. For the Ste5[ND] strain, we observed a weak, although not zero, signal for all concentrations of α-factor. The switch-like decision also occurs rapidly: the steady-state level of the Fus3–Ste5 complex is invariant after 2 min of treatment with pheromone (Supplementary Figs 8 and 18).

How is the dissociation of the Fus3–Ste5 complex modulated? Dephosphorylation of T287, a substrate of Ste5-bound Fus3, partly relieves inhibition of the mating response[9]. We proposed that full relief and dissociation of the Fus3–Ste5 complex could require dephosphorylation of other sites. On Ste5, we identified three other potential MAPK phosphorylation sites within a peptide (Ste5_pep2; residues 214–334) that binds to Fus3 with the same affinity as Ste5 and contains T287 (ref. 9) (Fig. 2b). In an *in vitro* kinase assay, Ste5 peptides (Ste5_pep2) in which all but one of the putative phosphosites were mutated to a non-phosphorylatable form were phosphorylated by Fus3 (Supplementary Fig. 9). Further, the switch-like dissociation of Fus3 from Ste5 requires the kinase activity of Fus3 (Fig. 2a) as the Fus3–Ste5 complex is independent of α-factor with kinase-dead Fus3 (K42R).

The steady-state levels of the Fus3–Ste5 complex are linearly proportional to the number of phosphosites on Ste5. We systematically mutated each phosphosite on Ste5 to be non-phosphorylatable (Ser to Ala and Thr to Val) individually (−1PS) and as combinations of two (−2PS), three (−3PS) and all four sites (−4PS). We then measured the Fus3–Ste5 complex using Rluc protein-fragment complementation assay in cells either not treated or treated with α-factor (1 μM) (Fig. 2c and Supplementary Fig. 10b). Our results demonstrate that α-factor can induce a change in the steady-state levels of the Fus3–Ste5 complex if any individual site on Ste5 can be phosphorylated and that complete mutation of all sites (−4PS) is equivalent to Ste5[ND].

[1]Département de Biochimie, [2]Centre Robert-Cedergren, Bio-Informatique et Génomique Université de Montréal, C.P. 6128, Succursale centre-ville Montréal, Québec H3C 3J7, Canada. [3]Department of Mathematics, Imperial College London, South Kensington Campus, London SW7 2AZ, UK. [4]Department of Physiology, McGill University, 3655 Promenade Sir William Osler, Montréal, Québec H3G 1Y6, Canada. [5]Centre for Systems Biology at Edinburgh, University of Edinburgh, Edinburgh EH9 3JD, UK.
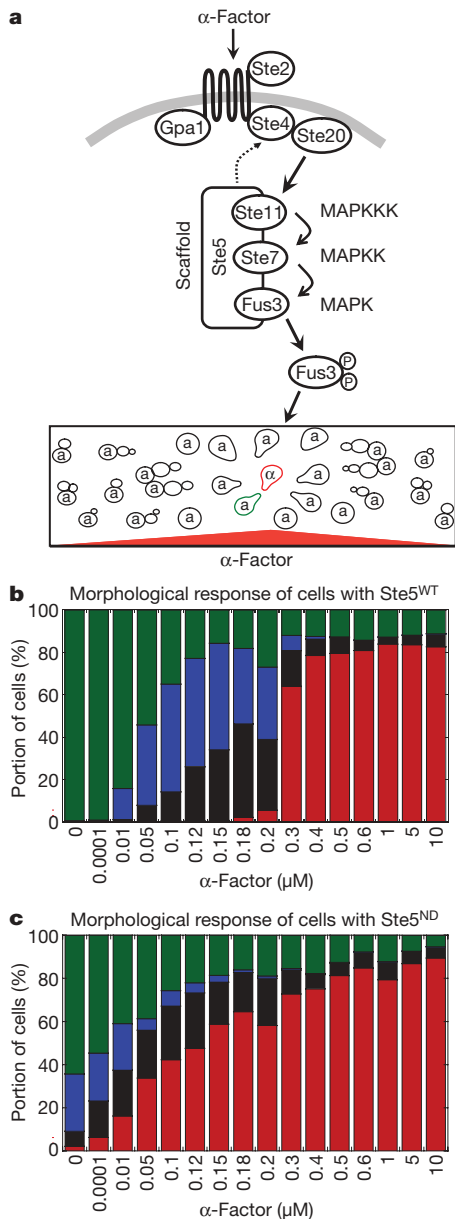*These authors contributed equally to this work.

Figure 1 | Switch-like shmooing in yeast requires the Fus3–Ste5 interaction. a, In *MATa* cells, α-factor pheromone activates a MAPK cascade that generates phosphorylated, active Fus3, which dissociates from Ste5 (ref. 30) and phosphorylates downstream targets to mediate mating[3]. Bottom panel: a *MATα* cell (red) secretes α-factor. Surrounding *MATa* cells display different morphologies determined by the α-factor concentration sensed. The *MATa* cell sensing a critical concentration of α-factor (green) 'shmoos' and mates with the *MATα* cell[2]. **b, c,** The fraction of different morphologies observed in *MATa ste5Δ* cells expressing either wild-type Ste5 (Ste5[WT]) (**b**) or the Ste5[ND] mutant (**c**). Morphologies: axial (green) or bipolar (blue) budding, arrested (black) and shmooing (red).

Dephosphorylation of all four sites is therefore sufficient to disrupt the Fus3–Ste5 complex and result in full activation of Fus3 (Supplementary Fig. 10c). Pseudo-phosphorylation of the four sites (Ser or Thr to Glu mutations) as individuals (+1PS), combinations of two (+2PS), three (+3PS) and all four sites (+4PS) in 0PS (or −4PS) protein suggests that Fus3 dissociates from Ste5 and becomes fully active only when all four sites are dephosphorylated (Fig. 2d and Supplementary Figs 11 and 12). If there is at least one pseudo-phosphorylation of Ste5, Fus3 is never fully activated and is unaffected by α-factor (Supplementary Fig. 11c). Our phosphosite mutants did not affect the expression or cellular localization of Ste5 (Supplementary Figs 13 and 14).

We next postulated that Ste5 must be dephosphorylated by a phosphatase whose activity at Ste5 is α-factor dependent. We identified a serine/threonine phosphatase Ptc1 that is essential for shmooing (Supplementary Fig. 15). The interaction of Ptc1 with Ste5 is α-factor dependent, and the levels of the Fus3–Ste5 complex are independent of α-factor in a *ptc1Δ* strain (Fig. 2e). Deletion of Ptc1 substantially prevents shmooing and reduces activation of Fus3, whereas its overexpression enhances both (Supplementary Fig. 15b, c). Ptc1 acts neither indirectly through the MAPK Hog1, a known substrate[12,13], nor directly through Fus3 (Supplementary Figs 16 and 17).

Our results suggest that α-factor induces recruitment of Ptc1 to Ste5, dephosphorylation of Ste5 and the consequent dissociation of the Fus3–Ste5 complex within the same time-frame (Fig. 2e and Supplementary Fig. 18). *In vitro*, Ptc1 was found to compete with Fus3 for the Ste5 phosphosites (Supplementary Fig. 19). Recruitment of Ptc1 occurs through a four-residue motif (amino acids 277–280) on Ste5, within the same region as the phosphosites, that when mutated to alanine (Ste5[AAAA]) prevents association of Ptc1 to Ste5 and, although not affecting Fus3–Ste5 binding, does prevent the dissociation of the Fus3–Ste5 complex with a concomitant loss of shmooing (Supplementary Figs 20 and 21). In our phosphosite mutants of Ste5, changes in levels of the Fus3–Ste5 complex and the shmooing response were insensitive to either the presence or absence of Ptc1 (Supplementary Fig. 22).

To understand how recruitment of Ptc1 to Ste5 (with a Hill coefficient ~2; Fig. 2e), and a change in the phosphorylation state of Ste5, generates a switch-like decrease in the levels of the Fus3–Ste5 complex (Hill coefficient >6; Fig. 2a), we examined potential mechanisms by mathematical modelling with a reduced system of differential equations, including only Ste5, Ptc1 and Fus3 (Fig. 3).

Switching could be partly explained by 'steric hindrance': the competition between Fus3 and Ptc1 for the phosphorylation of the four phosphosites on Ste5 (ref. 14). The linear relation between the degree of Ste5 phosphorylation and its affinity for Fus3 (Fig. 2c, d) indicates that the capacity of Fus3 to compete with Ptc1 is reduced as Ptc1 is recruited to Ste5. Consequently, the rate of dephosphorylation increases ultrasensitively with increasing concentrations of phero-mone. However, the sharpness of the switch generated is not compatible with our data.

We propose a robust zero-order ultrasensitivity mechanism based on a novel 'two-stage' binding of Fus3 and Ptc1 to Ste5 that can generate sufficient ultrasensitivity when coupled to steric hindrance. In our model, the enzymes are locally saturated, or at 'zero-order', because both Fus3 (ref. 9) and Ptc1 must first bind to separate docking motifs on Ste5 and only then can bind to and catalyse transformations of the phosphosites (Fig. 3a and Supplementary Fig. 23). This two-stage binding causes the competition between Fus3 and Ptc1 to be mostly insensitive to their cytosolic concentrations: locally, at each Ste5, the enzymes are saturated because the ratio of the substrate (the phosphosites) to the enzymes can be 4:1 (Fig. 3a). With both enzymes working near saturation, the level of phosphorylated Ste5 is very sensitive to a change in concentration of either enzyme[15,16]. When the concentration of pheromone reaches a threshold, a small increase in the levels of recruited Ptc1 will cause a large increase in unphosphorylated Ste5 because Fus3 is locally saturated and unable to compete with Ptc1, which is itself working near its maximum rate (Supplementary Fig. 24). Consequently, there is a sharp, ultrasensitive drop in the level of phosphorylation of Ste5 (Fig. 3b), reducing the affinity of Fus3 to Ste5 (Fig. 2c, d), and Fus3 undergoes a switch-like dissociation (Fig. 2a).

Our model predicts that the observed ultrasensitivity is generated by multi-site phosphorylation, two-stage binding and steric hindrance. We examined each in turn. First, if there is only one phosphosite on Ste5, the enzymes are not locally saturated at each Ste5 (Supplementary Fig. 25a), and there is little steric hindrance of Ptc1 because Fus3 binds weakly to Ste5 (Fig. 2c). Consequently, the
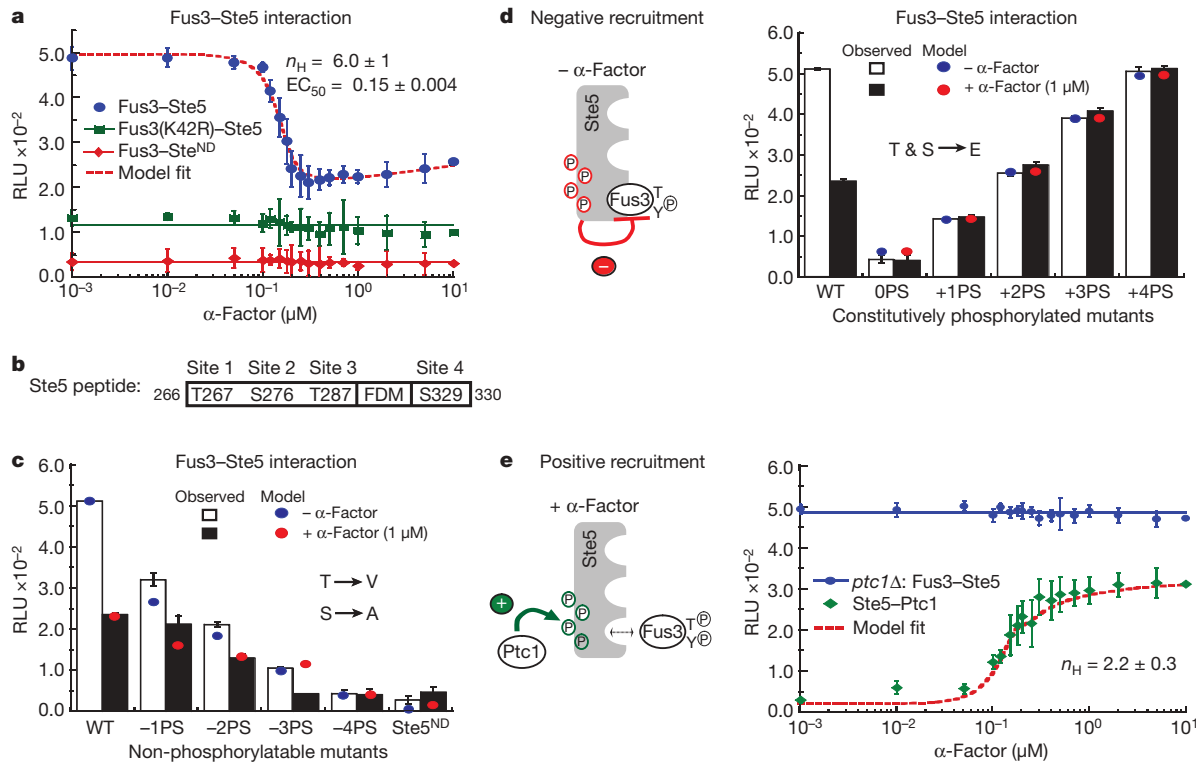
Figure 2 | Levels of the Fus3–Ste5 complex are determined by the Ste5 phosphorylation state. a, Steady-state levels of Fus3–Ste5, Fus3–Ste5ND and kinase-dead Fus3(K42R)–Ste5 versus α-factor. Model fit: dashed line. RLU, relative luminescence units. **b**, Ste5 peptide (residues 226–230) with four MAPK phosphorylation sites. **c**, Levels of Fus3–Ste5 complex with non-phosphorylatable phosphosites on Ste5. WT, wild-type Ste5. Red and blue circles: model predictions. **d**, As in **c**, for pseudo-phosphorylated Ste5. Red and blue circles: model fits. **e**, Fus3–Ste5 (*ptc1*Δ cells) and Ste5–Ptc1 (wild-type cells) interactions versus α-factor. Dashed red line: model fit. Hill coefficient (n_H), EC$_{50}$ values and their errors were calculated from fits to a Hill equation. Error bars, s.e.m. ($n = 3$).

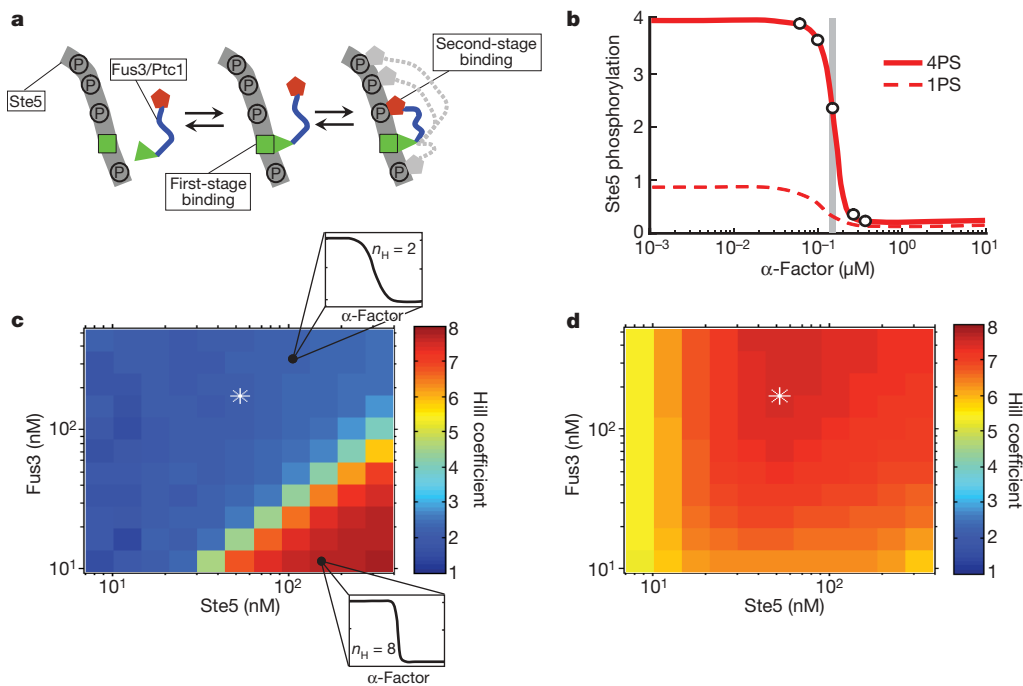**Figure 3 | A novel form of ultrasensitivity explains the switch-like mating decision. a**, Two-stage binding: Fus3 or Ptc1 first bind to their Ste5 docking sites (green) and then bind to individual phosphosites (red and grey enzyme domains). **b**, Steady-state Ste5 phosphorylation (open circles) versus α-factor for Ste5 with four (solid) or one (dashed) phosphosites. Grey bar: threshold concentration of α-factor. **c**, Predicted Hill coefficients for classic zero-order ultrasensitivity determined from Ste5 phosphorylation during α-factor dose–responses at fixed concentrations of Fus3 and Ste5 (insets). Asterisk: physiological Fus3 and Ste5 concentrations. **d**, As in **c**, for full two-stage binding and the steric hindrance model of Supplementary Fig. 23b.

sharpness of the switch is reduced (Fig. 3b). Second, eliminating two-stage binding of Ptc1 and Fus3 to Ste5 can give classic zero-order ultrasensitivity[15], but only at non-physiological concentrations of Ste5 (Fig. 3c). Finally, two-stage binding or steric hindrance alone will give a Hill coefficient of 4–5 (Supplementary Fig. 25b, c); however, if we include both we obtain the high Hill coefficients consistent with our data at physiological and a wide range of Fus3 and Ste5 concentrations (Fig. 3d and Supplementary Fig. 26).

Consistent with the predictions of our model, we confirmed that the sharpness of the switch is robust to changes in the concentration of Ptc1 for both the binding of Fus3 to Ste5 and the fraction of cells that shmoo, and that the sharpness of the Fus3–Ste5 interaction and the shmoo response is controlled by the number of active phospho-sites (Fig. 4 and Supplementary Figs 26 and 27).

We can speculate how the phosphorylation-dependent change in affinity of Ste5 for Fus3 occurs: either the negative charge of the phosphate groups on Ste5 or a known conformation change in a domain of Ste5 directly affects the binding of Fus3 (refs 17–20). Further, we need to understand how α-factor-mediated binding of Ptc1 to the phosphosites on Ste5 is enhanced. Two possibilities are that upon its membrane recruitment, Ste5 undergoes conformation changes that increase the accessibility of the phosphosites to Ptc1, or simply that the local concentration of Ptc1 at Ste5 increases at the membrane[3,17]. Finally, why are individual cells with Ste5[ND] always found in one of the four morphological states? It is possible that there are other switches downstream of the Fus3–Ste5 switch, with thresholds that vary stochastically across a population of cells. Such variation is only revealed by the graded activation of Fus3 generated by Ste5[ND]. Although specific switching mechanisms are unknown, there is a precedent for feedback generating ultrasensitive and bistable responses[4,17,21].

Multiple phosphorylation sites are common[22,23]. As well as generating ultrasensitivity in cascades of enzymes[11], potentially allowing

proofreading of substrates[24] and determining binding specificity[18,25], our results provide another function: generating robust, switch-like cellular decisions. Scaffold proteins are found in many eukaryotic signalling pathways, and scaffolded MAPKs are central to diseases including cancers, inflammatory disease, obesity and diabetes[26,27]. If similar mechanisms to the one we have discovered occur in mammalian signalling, they could prove to be important targets for therapeutic intervention.

METHODS SUMMARY

Plasmid constructions, cloning and gene manipulations were performed using standard methods. The mathematical model was constructed using the Facile network compiler with a rule-based modelling scheme to generate a description of the model as a set of differential equations[28]. The model was integrated in Matlab (Mathworks) and parameters were fitted using an efficient Markov chain Monte Carlo method[29]. Detailed experimental, modelling and simulation methods are described in Supplementary Information.

1. Darwin, C. *The Descent of Man, and Selection in Relation to Sex* (John Murray, 1871).
2. Jackson, C. L. & Hartwell, L. H. Courtship in *S. cerevisiae*: both cell types choose mating partners by responding to the strongest pheromone signal. *Cell* **63**, 1039–1051 (1990).
3. Elion, E. A. Pheromone response, mating and cell biology. *Curr. Opin. Microbiol.* **3**, 573–581 (2000).
4. Paliwal, S. *et al.* MAPK-mediated bimodal gene expression and adaptive gradient sensing in yeast. *Nature* **446**, 46–51 (2007).
5. Pawson, T. & Scott, J. D. Signaling through scaffold, anchoring, and adaptor proteins. *Science* **278**, 2075–2080 (1997).
6. Burack, W. R. & Shaw, A. S. Signal transduction: hanging on a scaffold. *Curr. Opin. Cell Biol.* **12**, 211–216 (2000).
7. Erdman, S. & Snyder, M. A filamentous growth response mediated by the yeast mating pathway. *Genetics* **159**, 919–928 (2001).
8. Hao, N. *et al.* Regulation of cell signaling dynamics by the protein kinase-scaffold Ste5. *Mol. Cell* **30**, 649–656 (2008).
9. Bhattacharyya, R. P. *et al.* The Ste5 scaffold allosterically modulates signaling output of the yeast mating pathway. *Science* **311**, 822–826 (2006).
10. Stefan, E. *et al.* Quantification of dynamic protein complexes using *Renilla* luciferase fragment complementation applied to protein kinase A activities *in vivo*. *Proc. Natl Acad. Sci. USA* **104**, 16916–16921 (2007).
11. Ferrell, J. E. Jr & Machleder, E. M. The biochemical basis of an all-or-none cell fate switch in *Xenopus* oocytes. *Science* **280**, 895–898 (1998).
12. Warmka, J. *et al.* Ptc1, a type 2C Ser/Thr phosphatase, inactivates the HOG pathway by dephosphorylating the mitogen-activated protein kinase Hog1. *Mol. Cell. Biol.* **21**, 51–60 (2001).
13. McClean, M. N., Mody, A., Broach, J. R. & Ramanathan, S. Cross-talk and decision making in MAP kinase pathways. *Nature Genet.* **39**, 409–414 (2007).
14. Salazar, C. & Hofer, T. Versatile regulation of multisite protein phosphorylation by the order of phosphate processing and protein-protein interactions. *FEBS J.* **274**, 1046–1061 (2007).
15. Goldbeter, A. & Koshland, D. E. Jr. An amplified sensitivity arising from covalent modification in biological systems. *Proc. Natl Acad. Sci. USA* **78**, 6840–6844 (1981).
16. Ferrell, J. E. Jr. Tripping the switch fantastic: how a protein kinase cascade can convert graded inputs into switch-like outputs. *Trends Biochem. Sci.* **21**, 460–466 (1996).
17. Strickfaden, S. C. *et al.* A mechanism for cell-cycle regulation of MAP kinase signaling in a yeast differentiation pathway. *Cell* **128**, 519–531 (2007).
18. Nash, P. *et al.* Multisite phosphorylation of a CDK inhibitor sets a threshold for the onset of DNA replication. *Nature* **414**, 514–521 (2001).
19. Serber, Z. & Ferrell, J. E. Jr. Tuning bulk electrostatics to regulate protein function. *Cell* **128**, 441–444 (2007).
20. Good, M. *et al.* The Ste5 scaffold directs mating signaling by catalytically unlocking the Fus3 MAP kinase for activation. *Cell* **136**, 1085–1097 (2009).
21. Peter, M. & Herskowitz, I. Direct inhibition of the yeast cyclin-dependent kinase Cdc28-Cln by Far1. *Science* **265**, 1228–1231 (1994).
22. Cohen, P. The regulation of protein function by multisite phosphorylation – a 25 year update. *Trends Biochem. Sci.* **25**, 596–601 (2000).
23. Holmberg, C. I., Tran, S. E., Eriksson, J. E. & Sistonen, L. Multisite phosphorylation provides sophisticated regulation of transcription factors. *Trends Biochem. Sci.* **27**, 619–627 (2002).
24. Swain, P. S. & Siggia, E. D. The role of proofreading in signal transduction specificity. *Biophys. J.* **82**, 2928–2933 (2002).
25. Lenz, P. & Swain, P. S. An entropic mechanism to generate highly cooperative and specific binding from protein phosphorylations. *Curr. Biol.* **16**, 2150–2155 (2006).
26. Hirosumi, J. *et al.* A central role for JNK in obesity and insulin resistance. *Nature* **420**, 333–336 (2002).
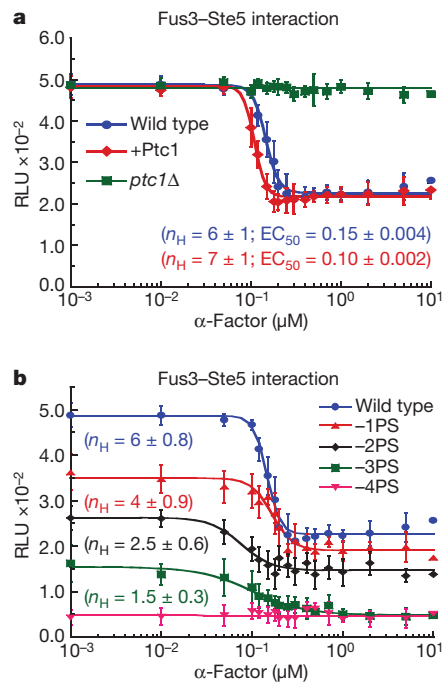

Figure 4 | Experimental validation of model predictions. a, Changes in the steady-state levels of the Fus3–Ste5 complex with various Ptc1 concentrations *in vivo*: wild type, knockout (*ptc1Δ*) and overexpression (+Ptc1). **b,** *In vivo* analysis of the steady-state levels of the Fus3–Ste5 complex as a function of α-factor using single (−1PS: AbCD), double (−2PS: abCD), triple (−3PS: Abcd) or quadruple (−4PS: abcd) non-phosphorylatable mutants of Ste5. The Hill coefficient (n_H), EC$_{50}$ values and their errors are calculated from fits of the data to a Hill function (solid lines). Error bars, s.e.m. (*n* = 3).

27. Lawrence, M. C. *et al.* The roles of MAPKs in disease. *Cell Res.* **18**, 436–442 (2008).
28. Siso-Nadal, F., Ollivier, J. F. & Swain, P. S. Facile: a command-line network compiler for systems biology. *BMC Syst. Biol.* **1**, 36 (2007).
29. Haario, H. M. L., Mira, A. & Saksman, E. DRAM: efficient adaptive MCMC. *Stat. Comput.* **16**, 339–354 (2006).
30. van Drogen, F., Stucke, V. M., Jorritsma, G. & Peter, M. MAP kinase dynamics in response to pheromones in budding yeast. *Nature Cell Biol.* **3**, 1051–1059 (2001).

Author Contributions M.K.M. and S.W.M. planned and designed experiments; M.K.M. performed experiments; V.S. and P.S.S. planned and V.S. performed the mathematical modelling; M.K.M., S.W.M., V.S. and P.S.S. analysed the results; M.K.M., V.S., P.S.S. and S.W.M. wrote the manuscript.

Author Information Reprints and permissions information is available at www.nature.com/reprints. The authors declare no competing financial interests. Correspondence and requests for materials should be addressed to S.W.M. (stephen.michnick@umontreal.ca) or P.S.S. (peter.swain@ed.ac.uk).